

Optimal Load Frequency Control of a Multi-Area Power System with Dead Band Effect and Generation Rate Constraints

Narender Saini^{1*}, Jyoti Ohri²

1- National Institute of Technology Kurukshetra, Kurukshetra, 136119, India.

Email: narender_61900104@nitkkr.ac.in (Corresponding author)

2- National Institute of Technology Kurukshetra, Kurukshetra, 136119, India.

Email: ohrijyoti@nitkkr.ac.in

Received: 4 October 2022

Revised: 7 November 2022

Accepted: 23 December 2022

ABSTRACT:

Load frequency control is an important factor of supplying quality electricity in an interconnected power system. As a result, an optimally tuned Proportional-Integral-Derivative (PID) controller is proposed in this work to eliminate frequency errors caused by unexpected load changes while maintaining tie-line power exchange. The PID controller is tuned using several optimization techniques such as GA, PSO, SCA, and GWO. A two-area power system with Generation Rate Constraint is studied in the first instance, and a three-area thermal power system with both generation rate constraint and dead band effect is considered in the second case. In both scenarios, a PID controller is employed for each area. When compared to the results of other optimization approaches for the same integrated power system, such as Genetic Algorithm, Particle Swarm Optimization, and Sine Cosine Algorithm, the GWO-based PID controller outperforms them in both scenarios. According to the simulation findings, the GWO technique gives better dynamic responses in terms of overshoot value, settling time, and Integral Time Absolute Error. Finally, to evaluate the robustness of the suggested optimization strategies, sensitivity analysis is done by modifying the system parameters (turbine time constant, governor time constant, and both simultaneously) in the range of 25% from their nominal values.

KEYWORDS: Load Frequency Control (LFC), PID Controller, Generation Rate Constraint, Frequency Deviation, Grey Wolf Optimization (GWO).

1. INTRODUCTION

One of the most challenging tasks in control engineering is the power system control, because there should be a balance between the total load demand and the total generated power in the presence of various electrical equipment such as generators, transmission lines, protection devices, and controller loops that generally spread in large geographical areas. The delivery of electricity to the fluctuating load is the major objective of the electrical power system. Any variations in load have the most significant impact on the network frequency of the power system. The initial power mismatch and the inertia of the system both have an effect on the rate at which the frequency deviates from the value that was set for it. Controlling the frequency of the load is one of the most essential tasks for providing effective management of the power system. LFC's primary objective is to keep frequency fluctuations to a minimum level by using controllers to achieve the desired level of symmetry between the power that is

demand and the power that is produced[1]. The three types of frequency controllers are classified as:

- Primary frequency control: - Operating time limits of primary frequency control is 2 to 20 sec. It may be divided majorly into
 - The Inertial response, also known as the quick response.
 - Governor response, called as a sluggish response.
- Secondary/supplementary frequency control: - This is usually known as AGC or LFC. Its operating time is 20 sec. to 2 min. Whenever imbalance occur between the load demand and generated power, it helps in maintaining the system's frequency and regulates the power exchange between the interconnected area.
- Tertiary frequency control: - In any large power system when there is a serious load-generation imbalance. In this situation, the tertiary control

comes into consideration to decrease the risk of faults[2]. Its operating time is above 10 min.

2. LITERATURE REVIEW

Various types of controller and techniques are designed throughout the last years for the LFC issue but still some improvement is to be needed in this. For the AGC of the multi-area power system, the idea of advanced optimum control was initially presented in[3]. The load frequency control problem for single area thermal power systems, single area multiunit systems, and single area hydropower system is presented in[4]–[7]. In the paper[8]–[17], the LFC for a multi-area power system is provided. Frequency control for the two area single source interconnected system is introduced in [9]–[11], [18]. In [12], the LFC of three area with reheat turbine and GRC effect is presented. Controller to reduce the frequency error and maintain the power exchanged in multi-area multiunit system is presented in[11], [12], [17]. PID as a supplementary controller is suggested for a five-area reheated thermal power plant in [19]. Various kind of controllers such as Fuzzy classical controller[8], PI controller [20]–[23], PID controller[19], [24], Type II fuzzy PID[14], Fractional order PID [15], [17], [25], Model Predictive Control (MPC) [25]–[28], Sliding mode control [29], [30] are commonly used in the AGC as a secondary/supplementary control to keep the frequency stable. Most of the researchers used conventional controllers for the LFC and it was observed that the controller's performance totally depends upon the selection of value of the controller parameters. So, the main task is to determine the optimal value of the controller's gain for the enhancement of their performance. In the past, classical approaches such as ZN etc., are used to tune the controller which are totally hit and trial methods. Because the power system has many non-linearities and load demand varies continuously, and these methods do not meet up the requirement. Therefore, we need some advanced methods which can work efficiently. To cop up with these difficulties heuristic and meta-heuristic approaches such as Particle Swarm Optimization (PSO) [31]–[33], Teaching Learning Based Optimization (TLBO) [10], Genetic Algorithm (GA)[13], [33], Bat algorithm (BA) [11], Backtracking Search Optimization *Algorithm* (BSA) [19], Ant-Lion Optimizer (ALO)[16], Salp Swarm Optimization (SSO) [14], Differential Evolution (DE), Imperialist Competitive Algorithm (ICA) [28], [34], Firefly Algorithm (FA) [19], Artificial Bee Colony (ABC)[24], and Bacterial Foraging Optimization Algorithm (BFOA)[35] Optimization, Ziegler-Nichols, fuzzy logic etc. are come into consideration. These meta-heuristic approaches are commonly employed by investigators due to their simplicity and avoidance of local optima.

Since the PID is the mostly used model independent controller to eliminate error from system and improve the system's performance, but its tuning (choosing the PID controller's gain) is a difficult process because the controller's performance is heavily dependent on the gains. As a result, calculating the perfect gain value is viewed as an optimization task, and different approaches are employed to find the best gain value. In this work, the performance of PID is going to be evaluated with four different optimization techniques PSO, SCA, GA, and GWO for controlling the frequency variations in multi area power system. Simulation results obtained from these optimization techniques are compared and it is observed that the GWO optimized PID controller gives better performance in comparison to others in all respects. The goal of this research was:

- To decrease the frequency fluctuations in the system being tested
- To determine the PID controller's optimal values by using PSO, SCA, GA and GWO algorithm.
- To investigate the robustness of the best method from the considered techniques by considering the random load pattern.

The aim is to investigate the robustness of the best among four in presence of uncertainties such as varying the system's parameters which are turbine and governor time constant and both at the same time by $\pm 25\%$.

The rest of the paper is as follows; Section 2 represents the test system and controller's modeling. Section 3 provides a quick overview of the GWO algorithm and other approaches. Simulation results obtained by GWO and other considered techniques are provided in the next section, and Section 5 has information about the upgraded model and its results. Lastly, section 6 concludes the paper

3. POWER SYSTEM MODEL

3.1. Two-area Power System

In this work, a two-area single unit power system model is considered in which each area has a rating of 2 GW with a nominal rating of 1 GW. In most of articles, physical constraints are not considered [36]. Taking into consideration all the physical constraints may be a difficult task and not useful too but some constraints, such as Generation Rate Constraints (GRC) must be considered to analyze the system's performance perfectly. If these constraints are not considered then the frequency and tie-line power variations could be nullified in a concise period, the considered system can also chase large disturbances in the load. But when these constraints are considered, system becomes non-linear and more deviations occur in the area control error. In the thermal power station, power cannot be generated immediately. It can generate power at a specified rate only (3-5%/min.), called GRC. So, in this work, the

effect of GRC is also considered to match the tested system with the practical scenario.

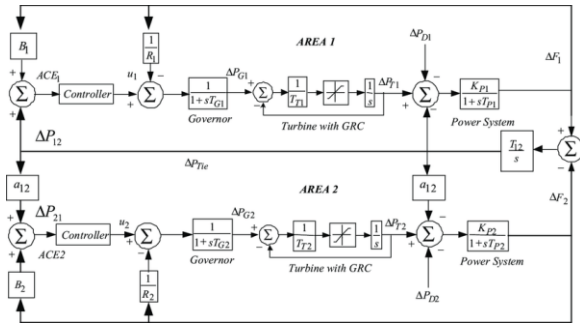


Fig. 1. Two area power system model.

The control input u_1 and u_2 are given as follow;

$$u_1 = K_{p1} ACE_1 + K_{i1} \int ACE_1 dt + K_{d1} \frac{d(ACE_1)}{dt} \quad (1)$$

$$u_2 = K_{p2} ACE_2 + K_{i2} \int ACE_2 dt + K_{d2} \frac{d(ACE_2)}{dt} \quad (2)$$

Table 1 lists the system's parameters for the test system.

Table 1. System's parameters for the test system.

$T_{T1} = T_{T2} = 0.3s$	$R_1 = R_2 = 2.4 \text{ HZ/p.u.}$
$T_{G1} = T_{G2} = 0.08s$	$B_1 = B_2 = 0.425 \text{ p.u.}$
$K_{P1} = K_{P2} = 120$	$T_{P1} = T_{P2} = 20s$
$a_{12} = -1$	$T_{12} = 0.545$

3.2. Random Change in Load Demand

Usually, the researchers considered the step change in load demand, but in this work, along with step change, a random load change has been considered. The variation that occurs in simulation is shown in the figure below. During the time interval of 0-50 sec. there is a step change of 1% (0.01 p.u) in power demand then in the period of 50-100 sec and 100-150 sec, step change of 3% and 2% are taken, respectively.

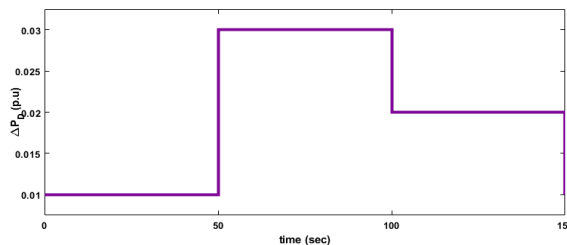


Fig. 2. Random change in power demand.

3.3. Controller and objective

Since there is an arbitrary change in the power demand due to which frequency deviates from its nominal value so as to sustain tie-line power exchange between related areas and manage frequency deviations, a controller is required so in this work, PID controller is employed in each area to solve the aforementioned issue. It is the most commonly used controller by researchers.

It helps in improving the system performance by minimizing the peak undershoot and overshoot in the response within significantly less time. The transfer function for the PID controller is

$$T_{pid} = K_p + \frac{K_i}{s} + K_d s \quad (3)$$

The PID controller functioning depends on gain parameters, so selection of optimal values of gain parameters is of utmost importance. In this work, GA, PSO, SCA, and GWO techniques are employed to accomplish this task. Whenever any unexpected load changes occur, the needed ACE in each area triggers the controller movement. The ACE signal is comprised of the incremental tie-line power and frequency change, and is given by

$$ACE_1 = B_1 \Delta f_1 + P_{tie12} \quad (4)$$

$$ACE_2 = B_2 \Delta f_2 + P_{tie21} \quad (5)$$

Where, Δf_1 and Δf_2 are change in system's frequency and P_{tie12} and P_{tie21} are incremental tie-line power.

In the frequency control, for the better functioning of the controller or system, the performance index (P.I) value should be minimum. Performance index value decides the controller's performance. Generally, four types of P.I are used, and ITAE is one of them and is chosen in this work. The ITAE expression is mainly composed of the frequency and the tie-line power change, as shown below.

$$P.I = ITAE = \int_0^{t_s} (|\Delta f_p| + |\Delta P_{tie-p-q}|) \cdot t dt \quad (6)$$

4. OPTIMIZATION TECHNIQUES

Various optimization techniques are employed in this work such as GA, PSO, SCA, and GWO to minimize the performance index given in (6) and optimize the controller performance for frequency control and sustain tie line power exchange despite physical limits in the thermal power system such as GRC and GDB. The brief introduction about the GWO is given below and other optimization techniques (SCA, PSO, GA) considered in this work are given in [37]–[39].

4.1. Grey Wolf Optimization

Mirjalili *et al.* developed GWO in 2014, a meta-heuristic method based on grey wolves' natural leadership and hunting behaviour. In the nature, they are thought to be apex predators and live in groups (packs). In a typical group, there are 8-14 members. Every member in the group has its significance. Alpha (α), Beta (β), Delta (δ) and Omega (ω) are the four levels of wolves in their group. The pack's leader is α , and they make all of the important choices. β are the subordinate wolves of alpha. Delta (δ) has to follow both α and β ,

but they control omega wolves [40]. Tracking the target, chasing and approaching it, surrounding and tormenting it until the prey comes to a complete stop, and then attacking the target are all part of the hunting process. The target's location is suggested by α , β , and δ , and then the remaining wolves, i.e., delta, in search of the fittest search agent renovate their place.

Mathematical model of GWO algorithm

The fittest solution is alpha, followed by beta, and finally delta in the GWO. Omega is the name for the rest of them. α , β , and δ generally direct the hunting process in the GWO algorithm and ω have to follow these three wolves. Following are the mathematical equations for encircling behavior:

$$D_p^{(i)} = |C_p \cdot P_{pq}^{*(i)} - P_{pq}^{(i)}| \tag{7}$$

$$P_{pq}^{(i+1)} = P_{pq}^{*(i)} - A_p \cdot D_p^{(i)} \tag{8}$$

Where

$p = 1, 2, 3, 4, 5 \dots M_p$ and $q = 1, 2, 3, \dots M$.

The following are the vectors A_p and C_p

$$A_p = 2a \cdot r_p - a \tag{9}$$

$$C_p = 2 \cdot r_p \tag{10}$$

Where,

Over the course of repetitions, the components of a are progressively lowered from 2 to 0. r_p is the random vectors in [0, 1].

Occasionally, the β and δ wolves participate in the hunting operation. As a consequence, α , β , and δ will have a better idea of where the prey is. The top three solutions α , β , and δ have been saved, and the remaining agents must renovate their locations to resemble the best search agents' place.

$$D_{\alpha q}^i = |C_1 \cdot P_{\alpha q}^i - P_{pq}^i| \tag{11}$$

$$P_{1q}^i = P_{\alpha q}^i - A_1 D_{\alpha q}^i \tag{12}$$

$$D_{\beta q}^i = |C_1 \cdot P_{\beta q}^i - P_{pq}^i| \tag{13}$$

$$P_{2q}^i = P_{\beta q}^i - A_2 D_{\beta q}^i \tag{14}$$

$$D_{\delta q}^i = |C_1 \cdot P_{\delta q}^i - P_{pq}^i| \tag{15}$$

$$P_{3q}^i = P_{\delta q}^i - A_3 D_{\delta q}^i \tag{16}$$

$$P_{pq}^{i+1} = \frac{P_{1q}^i + P_{2q}^i + P_{3q}^i}{3} \tag{17}$$

When the target's movement comes to a halt, the grey wolves attack it, bringing the search to a close. Wolves reach the target when A 's magnitude is smaller than 1, indicating an exploitation process. They split up to look for the prey and then converge in order to strike the target. When A has a magnitude greater than one, the wolves must move away from the objective in order to find alternative prey, a process known as exploration. The exploration process is also aided by Vector C . The random value in [0,2] is contained in vector C , as can be

seen from equation (10). As a result, GWO may do more random operations throughout the optimization process to encourage exploration while avoiding local optima.

The conclusion is that the search process begins by randomly generating the grey wolf population. Throughout the iteration, α , β , and δ approximate the target's predicted position. Each answer improves the distance between the prey and the predator. The exploitation and exploration were highlighted by the parameter 'a.' When the $|A|$ is more than 1, the solutions prefer to migrate away from the target, but when the magnitude of A is smaller than 1, the solutions tend to gather together to the prey. Finally, the GWO comes to an end when an end condition is met[40]. The flow chart for the GWO is shown in Fig. 3.

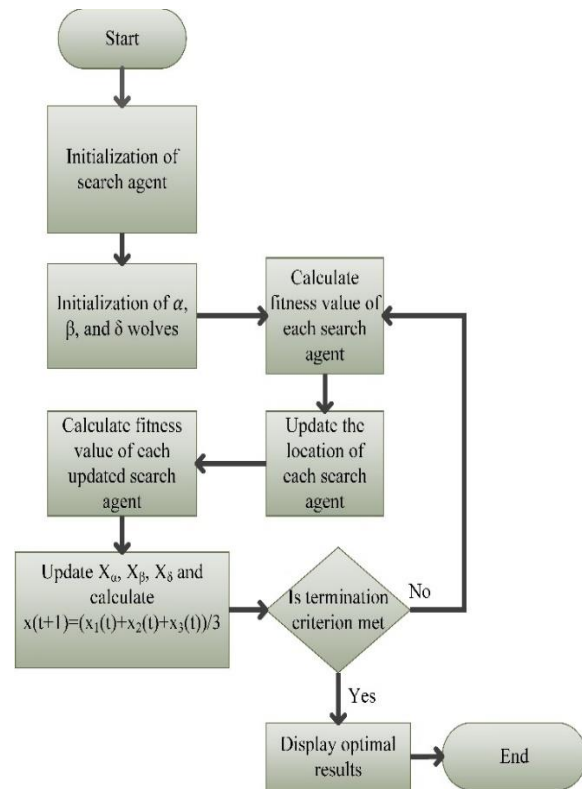


Fig. 3. Flow chart of GWO.

5. SIMULATION EXPERIMENT AND RESULTS

Model of a two-area power system with a non-reheat turbine and GRC undertaken for this study is shown in Fig.1. Two types of load changes are considered, one is step load change (0.01 p.u) and second is randomly load change shown in Fig. 2. The two-controller employed in each area is of PID type. The considered model is designed using the MATLAB (Simulink) platform.

5.1. System Response with 1% (0.01 p.u) Step Load Change in area-1

In this specific case, a step load variation of 1% (0.01 p.u.) in area-1 is taken into consideration. Within the

context of the optimization process, the ITAE plays the role of a goal. Because the GRC is such an essential aspect of LFC, its influence has been included into this model, and its value has been set at 0.0005 MW p.u./sec, which translates to 3 percent /min. The size of the population and the number of iterations are both set to 30. Each area has its own PID controller, and the GA, PSO, SCA, and GWO optimization algorithms are used to fine-tune these controller's settings. The final optimal gain values of the PID controller that were achieved via the application of the various optimization strategies that were explored are shown in Table 2 below.

Table 2. Controller parameters for different optimization.

Technique	Area-1			Area-2		
	K_P	K_I	K_D	K_P	K_I	K_D
GA	2.2315	0.8951	0.8886	1.1641	0.6937	0.6213
PSO	0.5394	0.0148	1.0	-0.8918	0.000001	0.0486
SCA	1.0	-0.0114	-0.0983	-0.7879	0.0015	0.0574
GWO	0.8085	0.5851	0.5047	0.0197	0.3202	0.00003

The convergence of the cost curve w.r.t the no. of iterations of different optimization techniques is shown in Fig. 4. The following figure demonstrates that GWO converges to minimum value in a very short range as compared to other techniques.

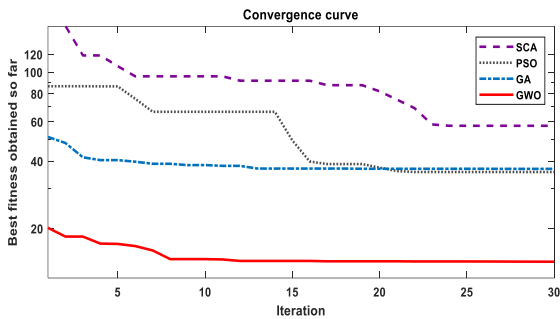


Fig. 4. Convergence curve of different optimization techniques.

Changes in frequency in both the areas i.e. Δf_1 and Δf_2 , and tie-line power ΔP_{tie} due to step load change obtained from the simulation experiment are displayed in Fig. 5 to Fig. 7, respectively. For the comparison purpose, the results obtained with other optimization techniques such as GA, PSO and SCA are also shown in these figures along with GWO.

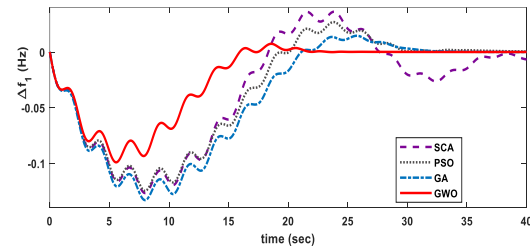


Fig. 5. Variations in frequency (Δf_1) in area-1 due to step load change.

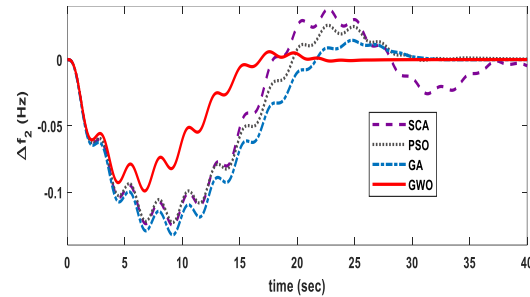


Fig. 6. Variations in frequency (Δf_2) in area-2 due to step load change .

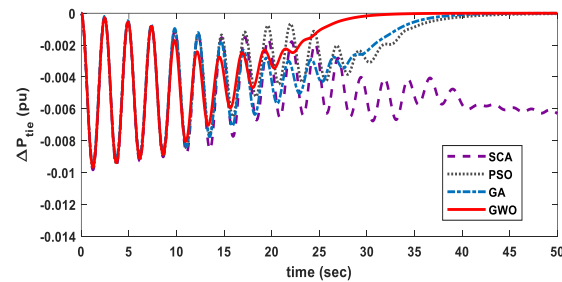


Fig. 7. Variations in tie-line power exchange (ΔP_{tie}) due to step load change.

Table 3 shows the ITAE, settling time (T_s), and maximum overshoot values derived from Fig. 3 to Fig. 7, respectively. Fig. 8 depicts the performance of the PID controller in terms of these performance indices obtained. Table 3 and Fig. 8 show that, when compared to GA optimized PID (ITAE=36.91), PSO optimized PID (ITAE=35.7275), and SCA optimized PID controller (ITAE=57.5035), the GWO optimized PID controller gives the lowest value for the objective function ITAE (14.1905). GWO optimized PID controller settles the frequency change (Δf_1 & Δf_2) and tie line power change (ΔP_{tie}) to minimum value faster as compared to others, the simulation run time (582) and the maximum overshoot value for the frequency change ($\Delta f_1=0.00736$, $\Delta f_2=0.00592$) and tie line power change ($\Delta P_{tie}=-0.00024$) are least in case of GWO based PID controller. So, in comparison to other explored techniques, the GWO optimized controller delivers a substantially better response in terms of settling times in tie-line power and frequency change, overshoot value, and simulation run duration.

Table 3. GWO performance compared based on error, overshoot value and settling time.

Technique	Settling time for			Maximum Overshoot for			ITAE	Simulation time per run (sec)
	Δf_1	Δf_2	ΔP_{tie}	Δf_1	Δf_2	ΔP_{tie}		
GA	30.401	29.774	37.994	0.01458	0.01457	-0.00019	36.91	56678
PSO	29.358	29.843	40.358	0.02690	0.02596	-0.00028	35.7275	1777
SCA	40.085	40.319	49.687	0.03614	0.03817	-0.00028	57.5035	1091
GWO	21.207	20.405	29.607	0.00736	0.00592	-0.00024	14.1905	582

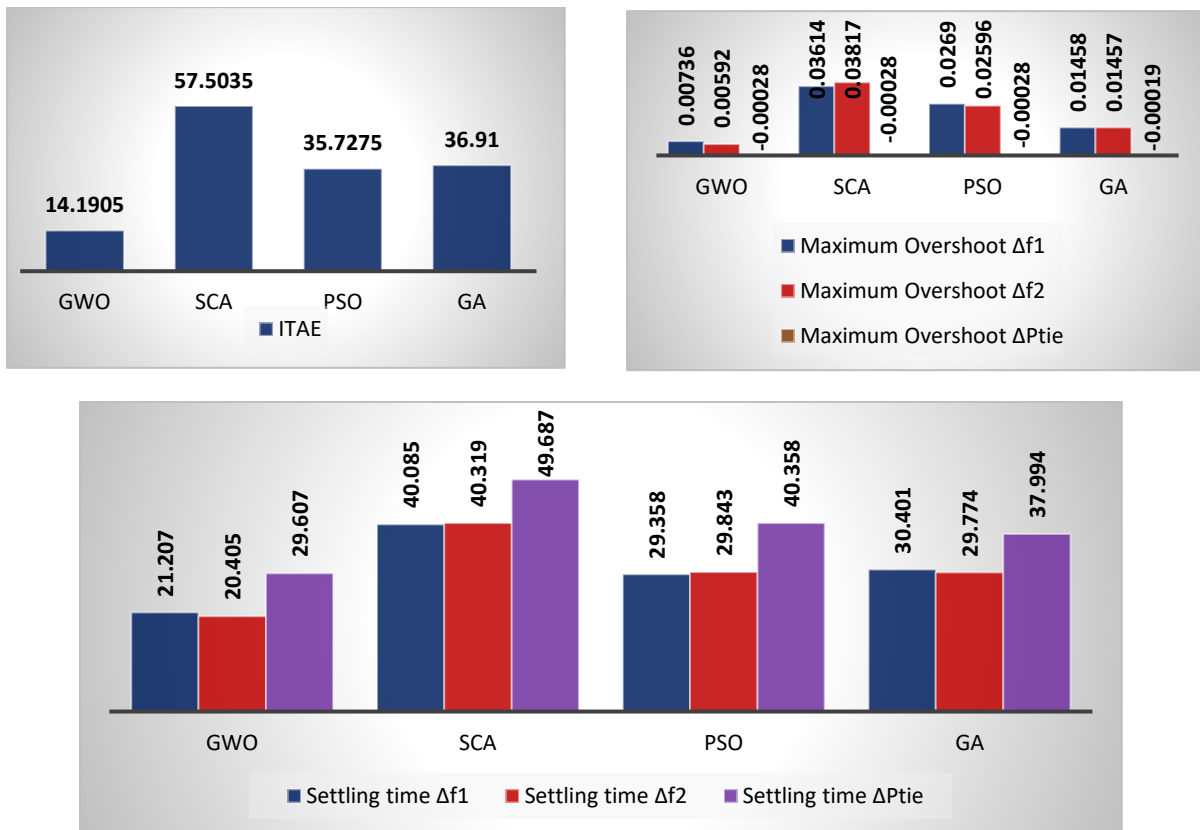


Fig. 8. Comparison of GWO based PID controller with other techniques.

5.2. System performance with random change in load

This simulation experiment is performed for the frequency control of a two-area single source system with random load changes depicted in Fig. 2 in area-1 using the GWO optimization approach. As it has been observed from the simulation experiment presented in section 4.1 that GWO gives the more superior performance and convergence than the other optimization techniques considered in this work. Hence the results obtained with GWO, are only shown in this section. The system response obtained for change in frequency (Δf_1 & Δf_2) in both areas and the tie line power (ΔP_{tie}) are shown in Fig. 9-11, respectively. Since the change in load is unexpected, it can

occur anytime so to check the effectiveness of the proposed approaches, random change in load is considered in area-1. The figures below demonstrate this clearly that GWO optimized PID controller has efficiently handled the random change in load demand and nullified the frequency error in very less time, and maintained the tie-line power exchange. The undershoot value and the oscillations in GWO optimized PID controller response are less as compared to other considered method.

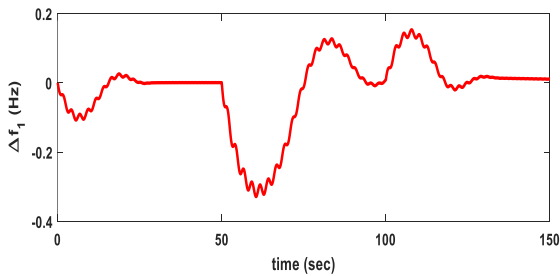


Fig. 9. Variations in frequency (Δf_1) in area-1 due to random load change.

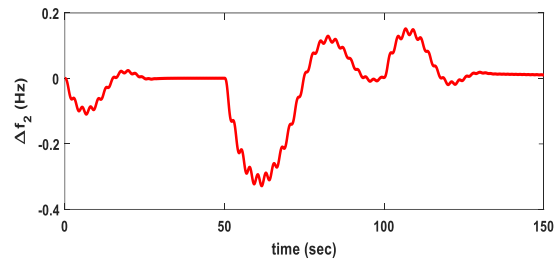


Fig. 10. Variations in frequency (Δf_2) in area-2 due to random load change.

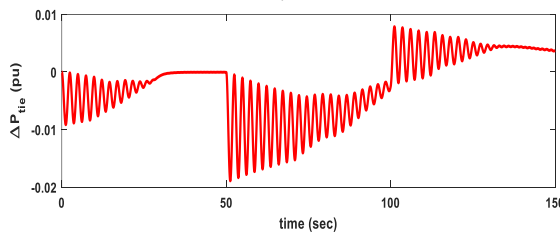


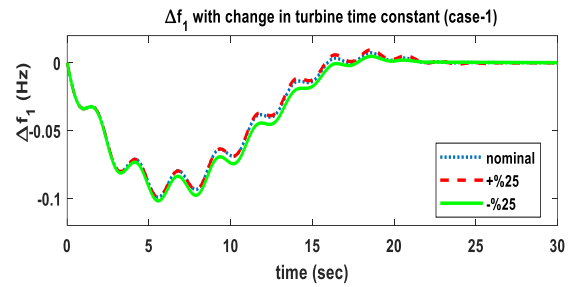
Fig. 11. Variations in tie-line power exchange (ΔP_{tie}) due to random load change.

5.3. Sensitivity Analysis

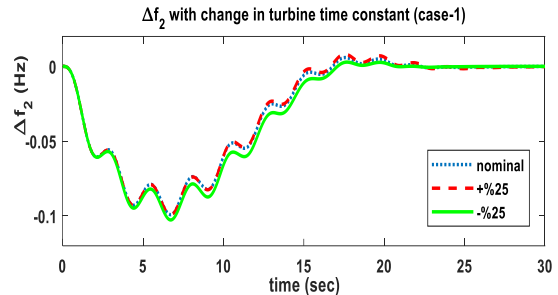
To test the resilience of the specified control mechanisms, a simulation experiment and sensitivity analysis are done. Three parameter uncertainty instances were examined.

- I. Case-1: - change in turbine time constant (T_T) up to $\pm 25\%$.
- II. Case-2: - change in governor time constant (T_G) up to $\pm 25\%$.
- III. Case-3: - The change in turbine and governor time constant up to $\pm 25\%$ are applied simultaneously.

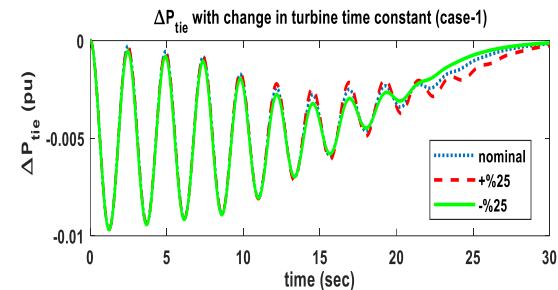
Under nominal conditions, the PID gains value obtained from the GWO optimization approach is preserved. As a result of the aforementioned scenarios, the system's parameters are changed to introduce the uncertainties. The PID gains value derived from the nominal condition are selected in this sensitivity analysis process for all the three cases of uncertainties. The frequency changes (Δf_1 & Δf_2) in both the areas and tie-line power change (ΔP_{tie}) for the above cases are shown in Fig. 12 to 14.



(a)

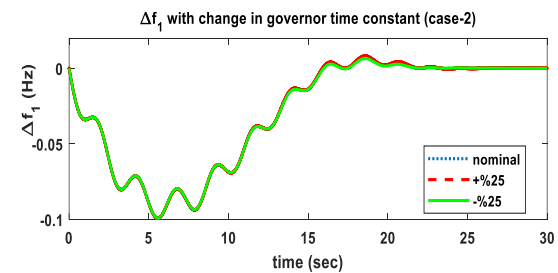


(b)

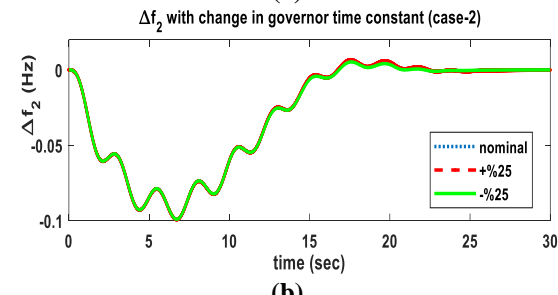


(c)

Fig. 12. Response of the tested system for case-1.



(a)



(b)

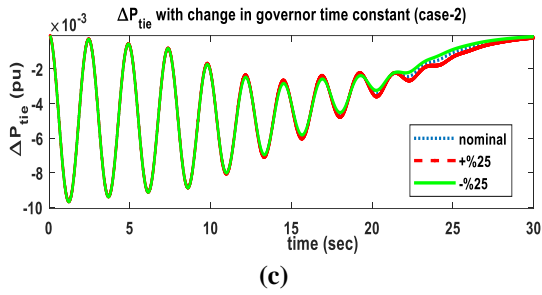


Fig. 13. Response of tested system for case-2.

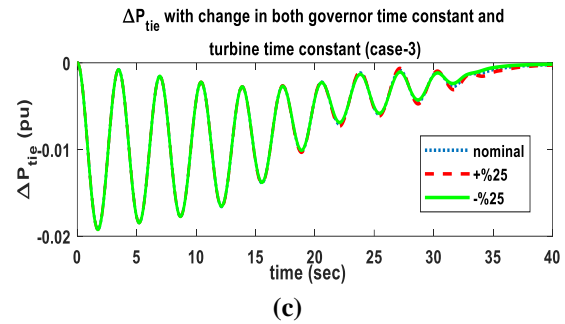
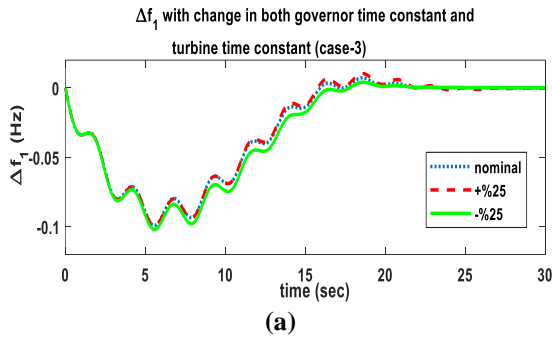
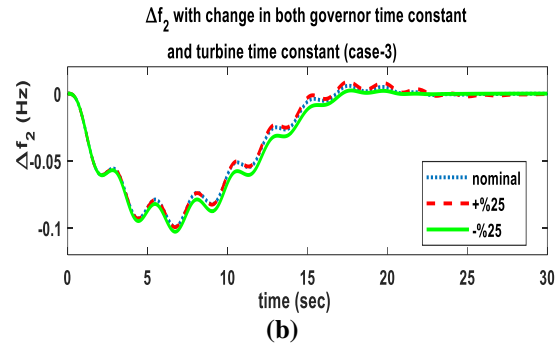
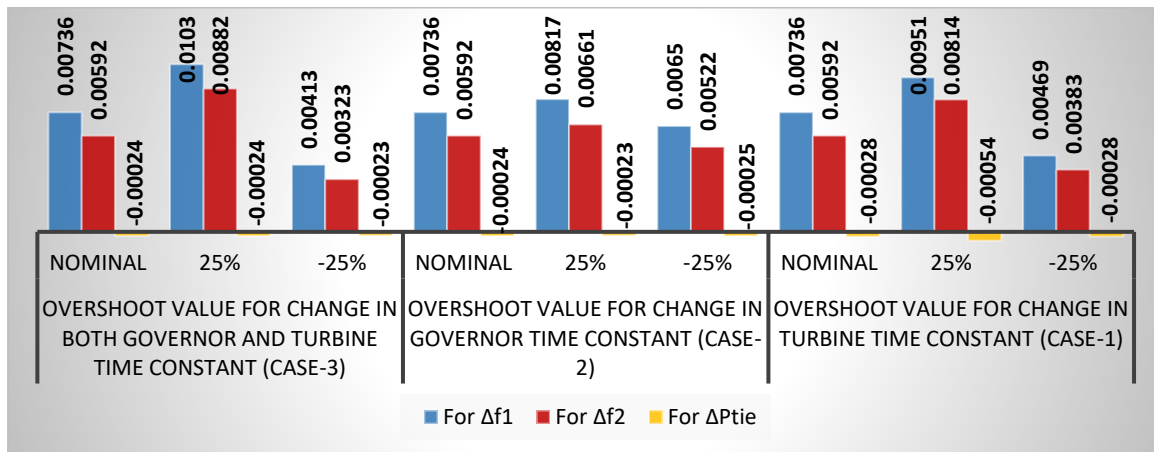


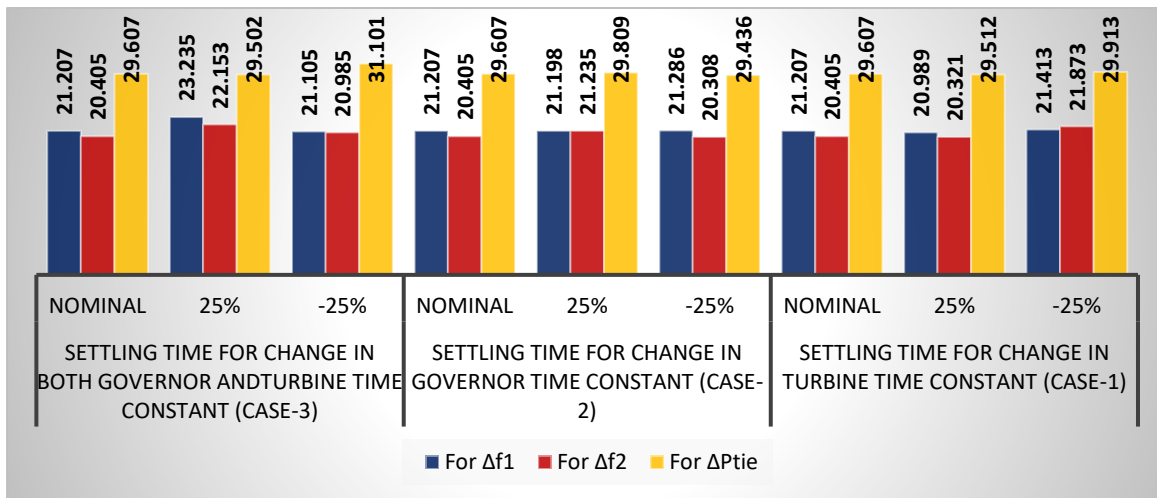
Fig. 14. Response of the tested system for case-3.

Table 4. Sensitivity analysis of the GWO optimization techniques.

		GWO		
		For Δf_1	For Δf_2	For ΔP_{tie}
Overshoot value for change in turbine time constant (case-1)	Nominal	0.00736	0.00592	-0.00028
	+25%	0.00951	0.00814	-0.00054
	-25%	0.00469	0.00383	-0.00028
Overshoot value for change in governor time constant (case-2)	Nominal	0.00736	0.00592	-0.00024
	+25%	0.00817	0.00661	-0.00023
	-25%	0.0065	0.00522	-0.00025
Overshoot value for change in both governor and turbine time constant (case-3)	Nominal	0.00736	0.00592	-0.00024
	+25%	0.0103	0.00882	-0.00024
	-25%	0.00413	0.00323	-0.00023
Settling time for change in turbine time constant (case-1)	Nominal	21.207	20.405	29.607
	+25%	20.989	20.321	29.512
	-25%	21.413	21.873	29.913
Settling time for change in governor time constant (case-2)	Nominal	21.207	20.405	29.607
	+25%	21.198	21.235	29.809
	-25%	21.286	20.308	29.436
Settling time for change in both governor and turbine time constant (case-3)	Nominal	21.207	20.405	29.607
	+25%	23.235	22.153	29.502
	-25%	21.105	20.985	31.101



(a)



(b)

Fig. 15. Change in (a) overshoot value and (b) settling time under parameter’s uncertainty.

From the response of the tested system for sensitivity analysis shown in fig. 12 to 14, it is observed that in spite of the uncertainties introduced in the system, the system performance does not deteriorate and it remains in the neighborhood of nominal value response. Table 4 shows the performance indices, such as overshoot values and settling time in each scenario for the GWO optimized controller based on the data collected from simulation results. For better understanding, the findings are shown in bar graph style in Fig. 15.

It can be seen from the Table 4 and the bar graph that the overshoot value and settling time vary within a very small range and the settling time in each case is almost similar. The results obtained from this sensitivity analysis proves that the controller ensures the robustness under the parameters uncertainty too.

6. THREE AREA POWER SYSTEM

To show the effectiveness of the GWO algorithm, the model is upgraded to three area thermal power

system as shown in Fig. 16. GRC and Governor Dead Band (GDB) are examples of non-linearity that must be taken into account when evaluating the system's performance in its whole. The rating of each unit in each area is 2GW, 4GW and 8GW. The shift in speed within which the governor valve position remains unchanged is called as governor dead band action. The GDB has a significant impact on the electrical power system's performance. In the system, it tends to create a sustained sinusoidal oscillation. The present work considered the backlash non-linearity of 0.05% ie. 0.03 (0.025 in case frequency is considered as 50 Hz). When GRC is used in combination with the GDB, the negative effect of GRC is amplified, and the system’s frequency may not achieve its nominal value within a certain time period. The parameters values and the reference model are taken from [10]. One PID controller is connected to settle down the frequency error. For tuning the PID controller, the same optimization techniques are employed in each area as used in the two-area power system above. A step

change in load of 1% (0.01 p.u) is considered at time t=0 in area-1 and in addition with the random load change

are also considered. The load variation considered is the random load change which is shown in Fig.2 above.

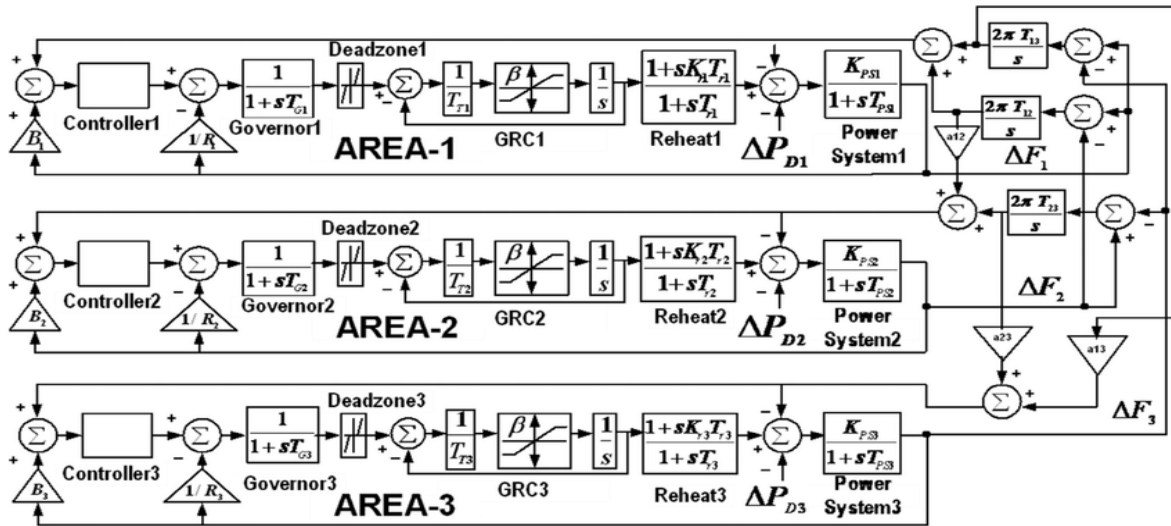


Fig. 16. Three unequal area -power system model.

6.1. Response of System with 1 % (0.01 p.u) Change in Load Demand

Table 5 shows the ideal gain settings for the PID controller for each area using the optimization

techniques discussed. The convergence of the cost curve with regards to the number of the iterations utilising the optimization approaches examined is depicted in Fig. 17.

Table 5. The PID controller's optimal gain value.

	Area-1			Area-2			Area-3		
	K _P	K _I	K _D	K _P	K _I	K _D	K _P	K _I	K _D
GA	1.7369	0.0883	0.4769	1.6169	0.3222	1.7012	0.7498	0.2245	0.9793
PSO	2.0	0.0693	0.9153	2.0	0.0842	2.0	0.1529	0.0809	0.0000011
SCA	-0.1278	0.0723	0.1513	0.6121	0.0765	-0.08917	0.5258	0.00378	0.23846
GWO	1.293	0.1169	1.3811	0.7790	0.1408	0.71711	1.626	0.10989	0.3495

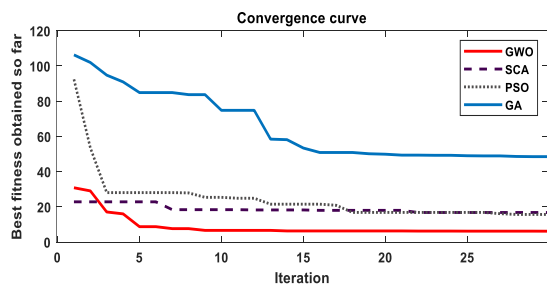
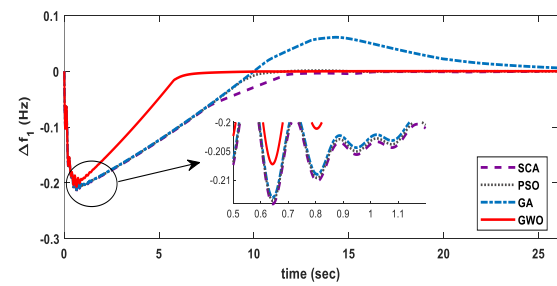
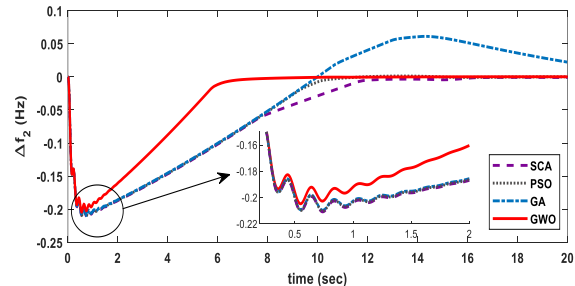


Fig. 17. Convergence curve of different optimization technique for three area power system.

The frequency deviation in all the three areas (Δf_1 , Δf_2 , and Δf_3) and tie-line power change (ΔP_{tie12} , ΔP_{tie13} , and ΔP_{tie23}) obtained from the simulation experiment using GWO optimized PID controller and other considered optimization-based controllers are shown in Fig. 17 to 19. From these figures, the settling time and the ITAE values are tabulated in the Table 6 below.



(a)



(b)

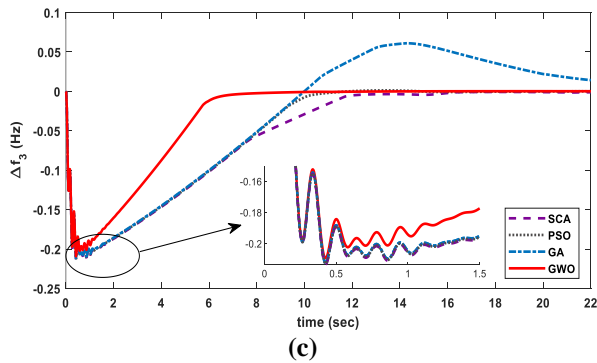


Fig. 18. Frequency change (a) Δf_1 in area-1 (b) Δf_2 in area-2 and (c) Δf_3 in area-3.

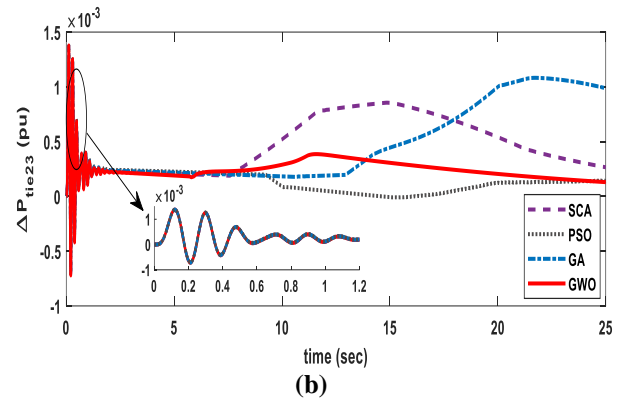
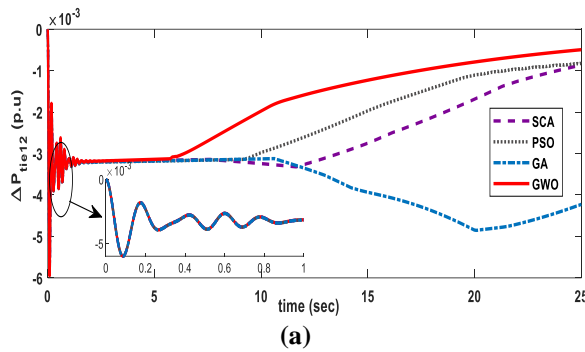


Fig. 19. Tie line power variation (a) ΔP_{tie12} within area-1 and area-2 (b) ΔP_{tie23} within area-2 and area-3 and (c) ΔP_{tie13} within area-1 and area-3.

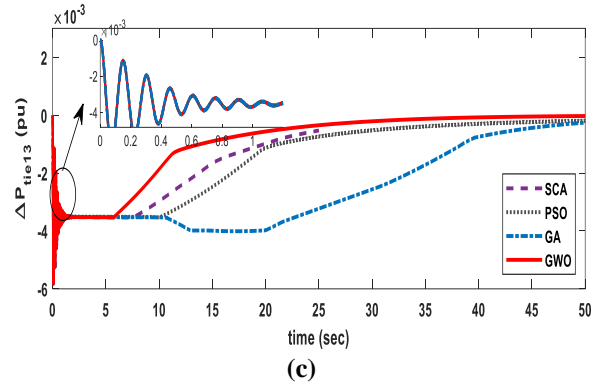


Table 6. Comparison of performance specification for three area system.

Technique	Settling time (sec) for						ITAE	Simulation run time
	Δf_1	Δf_2	Δf_3	ΔP_{tie12}	ΔP_{tie23}	ΔP_{tie13}		
GA	25.913	25.858	25.872	53.170	52.296	52.382	48.51	81543.76
PSO	10.326	10.328	10.305	40.621	38.3	39.644	15.672	4565.25
SCA	19.812	20.191	19.697	6.937	5.643	6.23	16.7872	2158.42
GWO	6.9071	6.9964	6.9671	37.539	38.279	34.909	6.1549	2386.38

It is observed from the Table 6 and above figures that the minimum value for ITAE (6.1549) is obtained from GWO optimized PID controller as compared to other techniques (GA=48.51, PSO=15.672, and SCA=16.7872). GWO optimized PID controller settles the frequency change in all three areas (Δf_1 , Δf_2 , and Δf_3) and tie line power change between all three areas (ΔP_{tie12} , ΔP_{tie13} , and ΔP_{tie23}) to minimum value faster as compared to other. It is observed that SCA gives lesser settling time for tie line power exchange as compared to GWO,

which gives far lesser setting time in frequency variations for all three areas and ITAE minimization. The simulation run time for the GWO (2386.38) and SCA (2158.42) is comparable and far lesser than GA and PSO. So, overall one can say that the GWO offers superior performance in terms of settling time, simulation run time, and minimizing the ITAE value than others. Below is the bar graph (Fig. 20) based on the above table for pictorial comparison.

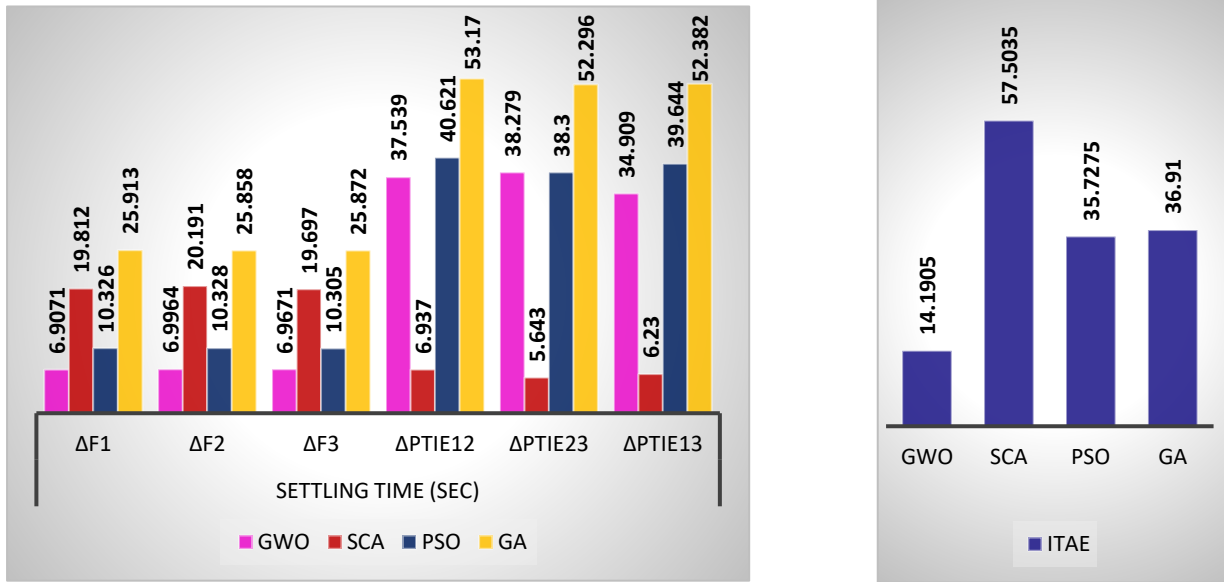


Fig. 20. Comparison of GWO based PID controller with other techniques for three area control.

6.2. Response of System with Random Load Change in area-1

To check the performance of GWO optimization based PID controller, a random load change as shown in Fig.2, is applied to area-1 and simulation experiment is performed. The system response obtained by PID controller for the frequency change and the tie line power change are shown in Fig. 21 to 22.

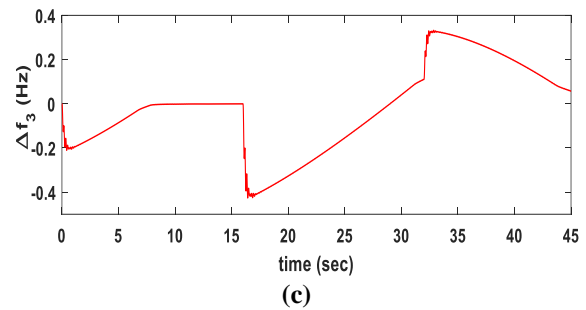
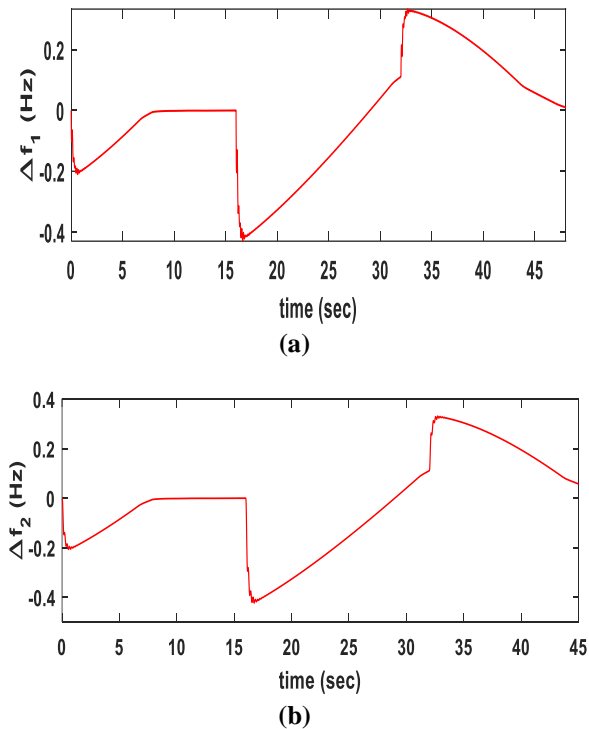
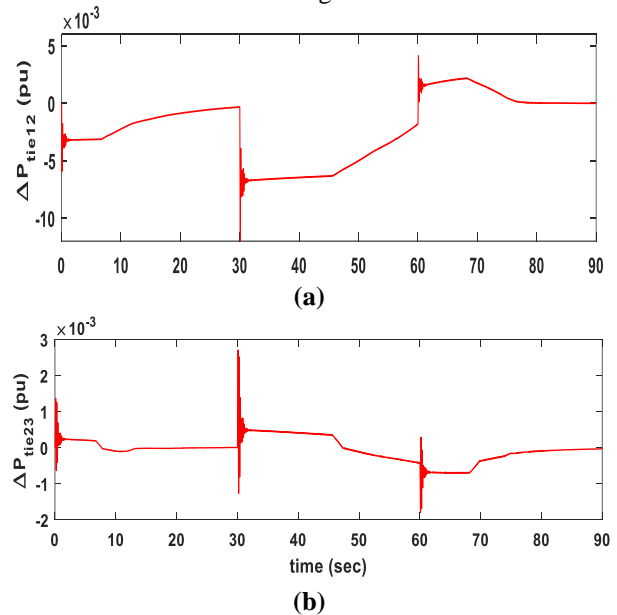


Fig. 21. Frequency variations (a) in area-1 (Δf_1), (b) in area-2 (Δf_2) and (c) in area-3 (Δf_3) with random load change.



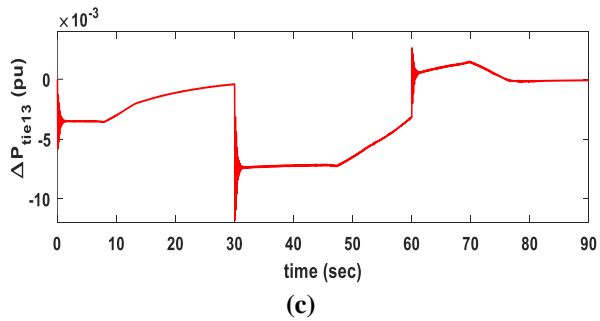


Fig. 22. Tie line power variation (a) within area-1 and area-2 (ΔP_{tie12}), (b) within area-2 and area-3 (ΔP_{tie23}) and (c) within area-1 and area-3 (ΔP_{tie13}) with randomly load change.

It is clearly seen from the Fig. 21 to 22 that GWO based PID controller is able to eliminate the fluctuation in the frequency of both areas and oscillations in the tie-line power in very little time which occurs due to the power demand changes with respect to time.

6.3. Sensitivity Analysis

Finally, to check the robustness of the GWO optimized controller for frequency control of three unequal area single unit power system, a sensitivity analysis is performed by varying the system’s parameters. Three cases of the parameter’s uncertainties have been considered as given in sec. 4.3. In the simulation process, the PID gains value calculated from the nominal condition are employed. The results obtained from the simulation experiment for the frequency change in all three areas are shown in Fig. 23 to 25 under the parameter’s uncertainties (governor time constant, turbine time constant and both together).

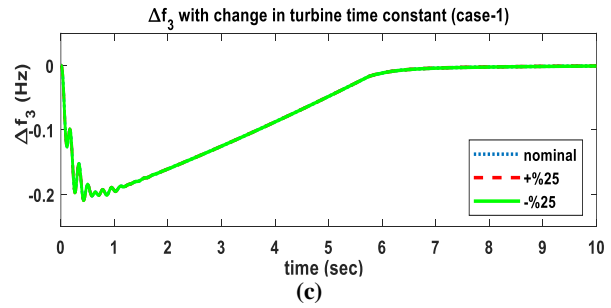
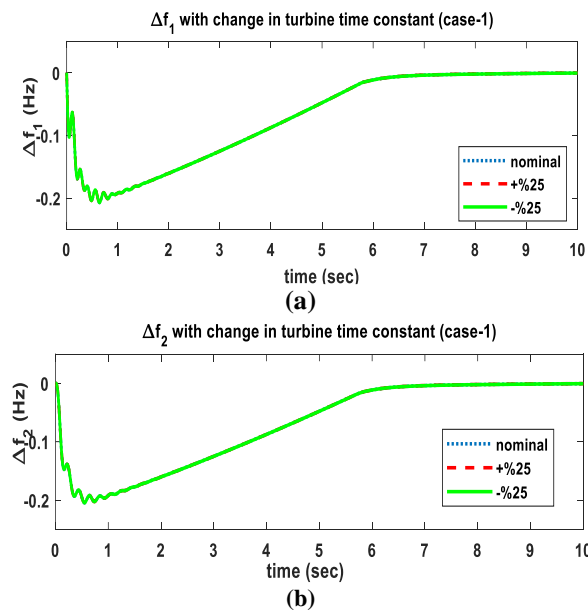


Fig. 23. Response of three area system for case-1.

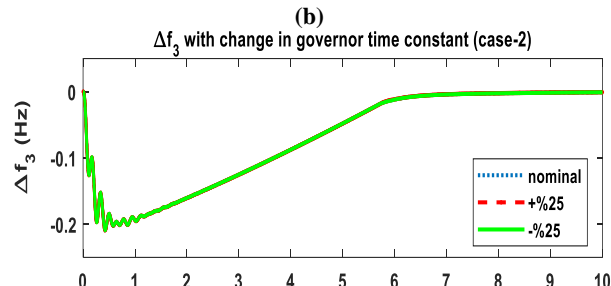
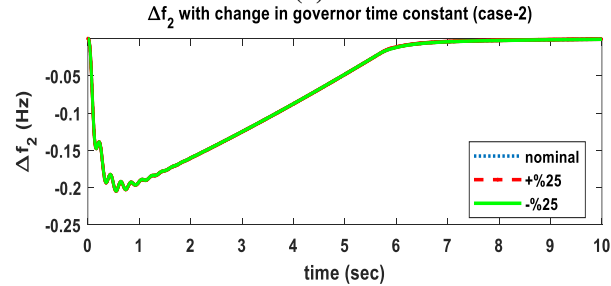
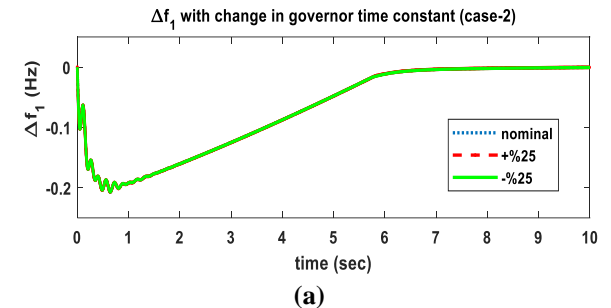
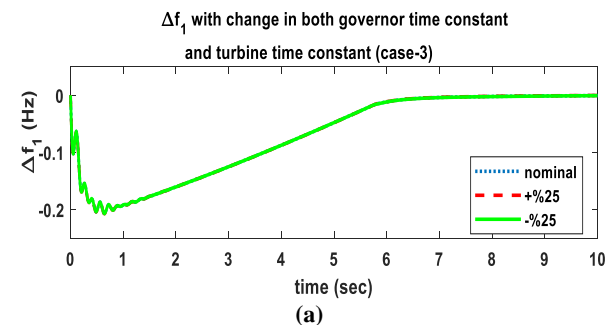


Fig. 24. Response of three area system for case-2.



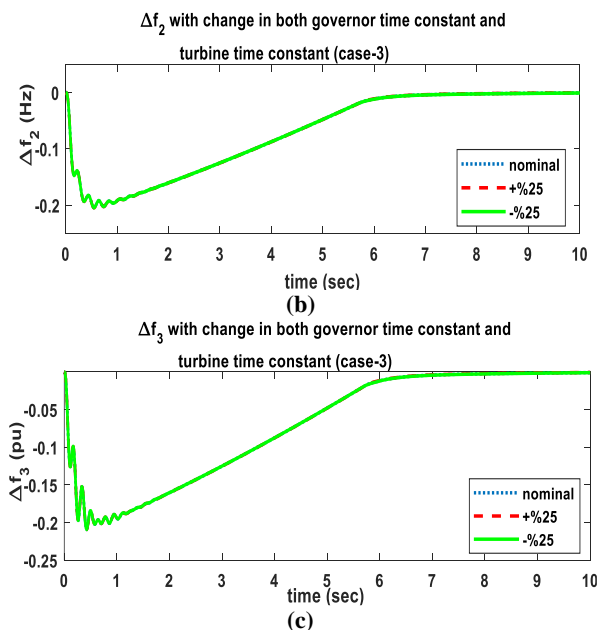


Fig. 25. Response of three area system for case-3.

Above figures show the robustness of the GWO optimized PID controller as it is clearly seen that the GWO is very efficient in controlling the frequency and the tie-line power deviations whenever changes occur in the system's parameters values and for large changes in the system's parameters, the optimal value of the controller's gains determined at the nominal condition with nominal parameters does not need to be reset.

7. CONCLUSION

The goal of LFC is to stabilize the tie-line power and frequency oscillations in the system. With the rising demand for electricity, it is more important than ever to have a robust LFC system that can handle system parameter uncertainty. GA, PSO, SCA, and GWO optimization techniques have been employed in this work to find the optimal values for the PID controller's gains for the LFC of multi-area power system. Two types of systems are considered. The first one is the two-area single unit with GRC effect, the second one is the three-area power system with GRC and dead band. Step load change of 1% (0.01 pu) and dynamic load change have been considered in area-1.

Better performance of GWO based PID controller is observed in LFC as compared to GA, PSO and SCA PID controller in terms of minimization of performance indices for two area system and three area system in presence of GRC and GDB. In addition to it, the robustness of the controller is also ascertained in the presence of uncertainties in system's parameters such as turbine and governor time constant individually and both simultaneously in the range of $\pm 25\%$ for both the systems. The simulation results reveal that the performance under parameter's uncertainties and normal

condition are more or less the same, the settling time value for the frequency error and tie-line power change vary within an acceptable range. Thus, the GWO optimized PID parameters obtained at nominal values are robust and stable.

8. NOMENCLATURE

- T_{12} \rightarrow Synchronizing coefficient.
- R_1 & R_2 \rightarrow Speed regulation parameters (p.u.).
- u_1 & u_2 \rightarrow Control inputs derived from the control outputs.
- P^*_{pq} \rightarrow The most satisfactory result obtained so far
- K_{p1} & K_{p2} \rightarrow Power system gain.
- t_s \rightarrow Simulation time.
- B_1 & B_2 \rightarrow Frequency bias parameters.
- ΔP_{D1} & ΔP_{D2} \rightarrow Change in load demand
- i \rightarrow Current iteration
- T_{t1} & T_{t2} \rightarrow Non-reheat turbine time constant (sec.).
- Δf_1 & Δf_2 \rightarrow Change in system frequency (Hz).
- T_{g1} & T_{g2} \rightarrow Speed governor time constant (sec.).
- ΔP_{tie} \rightarrow Tie-line power change (p.u.).
- A_p and C_p \rightarrow The coefficient vectors
- Δf_p \rightarrow Frequency change in p_{th} area
- T_{P1} & T_{P2} \rightarrow Power system time constants (sec.)
- ACE_1 & ACE_2 \rightarrow Area control errors.
- $\Delta P_{tie-p-q}$ \rightarrow Tie-line power change linking p_{th} and q_{th} area

REFERENCES

- [1] A. J. Wood and B. F. Wollenberg, *Power generation, operation, and control*. J. Wiley & Sons, 1996.
- [2] M. H. Soliman, H. E. A. Talaat, and M. A. Attia, "Power system frequency control enhancement by optimization of wind energy control system," *Ain Shams Eng. J.*, vol. 12, no. 4, pp. 3711–3723, Dec. 2021, doi: 10.1016/j.asej.2021.03.027.
- [3] O. I. Elgerd and C. E. Fosha, "Optimum Megawatt-Frequency Control of Multiarea Electric Energy Systems," 1970.
- [4] C. Ismayil, R. Sreerama Kumar, and T. K. Sindhu, "Automatic generation control of single area thermal power system with fractional order PID (PI λ D μ) controllers," in *IFAC Proceedings Volumes (IFAC-PapersOnline)*, 2014, vol. 3, no. PART 1, pp. 552–557. doi: 10.3182/20140313-3-IN-3024.00025.
- [5] K. P. S. Parmar, S. Majhi, and D. P. Kothari, "Load frequency control of a realistic power system with multi-source power generation," *Int. J. Electr. Power Energy Syst.*, vol. 42, no. 1, pp. 426–433, Nov. 2012, doi: 10.1016/j.ijepes.2012.04.040.
- [6] D. G. Padhan and S. Majhi, "A new control scheme for PID load frequency controller of single-area and multi-area power systems," *ISA Trans.*, vol. 52, no. 2, pp. 242–251, 2013, doi: 10.1016/j.isatra.2012.10.003.
- [7] S. Doolla and T. S. Bhatti, "Load frequency control of an isolated small-hydro power plant with reduced dump load," *IEEE Trans. Power Syst.*, vol. 21, no. 4, pp. 1912–1919, Nov. 2006, doi: 10.1109/TPWRS.2006.881157.
- [8] Y. Arya, "Automatic generation control of two-

- area electrical power systems via optimal fuzzy classical controller,” *J. Franklin Inst.*, vol. 355, no. 5, pp. 2662–2688, Mar. 2018, doi: 10.1016/j.jfranklin.2018.02.004.
- [9] H. Gozde and M. C. Taplamacioglu, “Automatic generation control application with craziness based particle swarm optimization in a thermal power system,” *Int. J. Electr. Power Energy Syst.*, vol. 33, no. 1, pp. 8–16, Jan. 2011, doi: 10.1016/j.ijepes.2010.08.010.
- [10] R. K. Sahu, T. S. Gorripotu, and S. Panda, “Automatic generation control of multi-area power systems with diverse energy sources using Teaching Learning Based Optimization algorithm,” *Eng. Sci. Technol. an Int. J.*, vol. 19, no. 1, pp. 113–134, Mar. 2016, doi: 10.1016/j.jestch.2015.07.011.
- [11] P. Dash, L. C. Saikia, and N. Sinha, “Automatic generation control of multi area thermal system using Bat algorithm optimized PD-PID cascade controller,” *Int. J. Electr. Power Energy Syst.*, vol. 68, pp. 364–372, 2015, doi: 10.1016/j.ijepes.2014.12.063.
- [12] Y. Sharma and L. C. Saikia, “Automatic generation control of a multi-area ST - Thermal power system using Grey Wolf Optimizer algorithm based classical controllers,” *Int. J. Electr. Power Energy Syst.*, vol. 73, pp. 853–862, Jun. 2015, doi: 10.1016/j.ijepes.2015.06.005.
- [13] A. Demiroren and H. L. Zeynelgil, “GA application to optimization of AGC in three-area power system after deregulation,” *Int. J. Electr. Power Energy Syst.*, vol. 29, no. 3, pp. 230–240, Mar. 2007, doi: 10.1016/j.ijepes.2006.07.005.
- [14] P. C. Sahu, S. Mishra, R. C. Prusty, and S. Panda, “Improved -salp swarm optimized type-II fuzzy controller in load frequency control of multi area islanded AC microgrid,” *Sustain. Energy, Grids Networks*, vol. 16, pp. 380–392, Dec. 2018, doi: 10.1016/j.segan.2018.10.003.
- [15] A. Delassi, S. Arif, and L. Mokrani, “Load frequency control problem in interconnected power systems using robust fractional PID controller,” *Ain Shams Eng. J.*, vol. 9, no. 1, pp. 77–88, Mar. 2018, doi: 10.1016/j.asej.2015.10.004.
- [16] M. Raju, L. C. Saikia, and N. Sinha, “Automatic generation control of a multi-area system using ant lion optimizer algorithm based PID plus second order derivative controller,” *Int. J. Electr. Power Energy Syst.*, vol. 80, pp. 52–63, Sep. 2016, doi: 10.1016/j.ijepes.2016.01.037.
- [17] J. Morsali, K. Zare, and M. Tarafdar Hagh, “Applying fractional order PID to design TCSC-based damping controller in coordination with automatic generation control of interconnected multi-source power system,” *Eng. Sci. Technol. an Int. J.*, vol. 20, no. 1, pp. 1–17, Feb. 2017, doi: 10.1016/j.jestch.2016.06.002.
- [18] M. Gupta, S. Srivastava, and J. R. P. Gupta, “A Novel Control Scheme for Load Frequency Control,” vol. 7, no. 2, pp. 31–40, 2013.
- [19] K. Jagatheesan, B. Anand, S. Samanta, N. Dey, A. S. Ashour, and V. E. Balas, “Design of a proportional-integral-derivative controller for an automatic generation control of multi-area power thermal systems using firefly algorithm,” *IEEE/CAA J. Autom. Sin.*, vol. 6, no. 2, pp. 503–515, Mar. 2019, doi: 10.1109/JAS.2017.7510436.
- [20] D. Guha, P. K. Roy, and S. Banerjee, “Application of backtracking search algorithm in load frequency control of multi-area interconnected power system,” *Ain Shams Eng. J.*, vol. 9, no. 2, pp. 257–276, Jun. 2018, doi: 10.1016/j.asej.2016.01.004.
- [21] A. Fathy and A. M. Kassem, “Antlion optimizer-ANFIS load frequency control for multi-interconnected plants comprising photovoltaic and wind turbine,” *ISA Trans.*, vol. 87, pp. 282–296, Apr. 2019, doi: 10.1016/j.isatra.2018.11.035.
- [22] M. R. Toulabi, M. Shiroei, and A. M. Ranjbar, “Robust analysis and design of power system load frequency control using the Kharitonov’s theorem,” *Int. J. Electr. Power Energy Syst.*, vol. 55, pp. 51–58, 2014, doi: 10.1016/j.ijepes.2013.08.014.
- [23] M. Mounica, C. D. Prasad, D. J. V. Prasad, and M. Aruna Bharathi, “Load frequency control of an isolated power system in presence of controllable energy storage devices,” *Majlesi J. Electr. Eng.*, vol. 12, no. 2, pp. 29–38, 2018.
- [24] K. Naidu, H. Mokhlis, and A. H. A. Bakar, “Multiobjective optimization using weighted sum Artificial Bee Colony algorithm for Load Frequency Control,” *Int. J. Electr. Power Energy Syst.*, vol. 55, pp. 657–667, 2014, doi: 10.1016/j.ijepes.2013.10.022.
- [25] M. M. Ismail and A. F. Bendary, “Load Frequency Control for Multi Area Smart Grid based on Advanced Control Techniques,” *Alexandria Eng. J.*, vol. 57, no. 4, pp. 4021–4032, Dec. 2018, doi: 10.1016/j.aej.2018.11.004.
- [26] A. M. Ersdal, L. Imsland, and K. Uhlen, “Model Predictive Load-Frequency Control,” *IEEE Trans. Power Syst.*, vol. 31, no. 1, pp. 777–785, Jan. 2016, doi: 10.1109/TPWRS.2015.2412614.
- [27] X. Sun, K. Liao, J. Yang, and Z. He, “Model Predictive Control based Load FrequencyControl for Power Systems with Wind TurbineGenerators,” 2019.
- [28] M. Elsisí, M. A. S. Aboelela, M. Soliman, and W. Mansour, “Model Predictive Control of Two-Area Load Frequency Control Based Imperialist Competitive Algorithm,” *TELKOMNIKA Indones. J. Electr. Eng.*, vol. 16, no. 1, pp. 75–82, 2015, doi: 10.11591/telkonnika.v15i3.8856.
- [29] J. Guo, “Application of full order sliding mode control based on different areas power system with load frequency control,” *ISA Trans.*, vol. 92, pp. 23–34, Sep. 2019, doi: 10.1016/j.isatra.2019.01.036.
- [30] B. H. Lai, A.-T. Tran, N. T. Pham, and V. Van Huynh, “Sliding Mode Load Frequency Regulator for Different-Area Power Systems with Communication Delays,” *J. Adv. Eng. Comput.*,

- vol. 5, no. 2, p. 93, Jun. 2021, doi: 10.25073/jaec.202152.323.
- [31] S. S. Dhillon, J. S. Lather, and S. Marwaha, “**Multi Area Load Frequency Control Using Particle Swarm Optimization and Fuzzy Rules,**” in *Procedia Computer Science*, 2015, vol. 57, pp. 460–472. doi: 10.1016/j.procs.2015.07.363.
- [32] N. K. Bahgaat, M. I. El-Sayed, M. A. M. Hassan, and F. A. Bendary, “**Load Frequency Control in Power System via Improving PID Controller Based on Particle Swarm Optimization and ANFIS Techniques,**” *Int. J. Syst. Dyn. Appl.*, vol. 3, no. 3, pp. 1–24, Oct. 2014, doi: 10.4018/ijdsda.2014070101.
- [33] S. K. Sinha, R. N. Patel, and R. Prasad, “**Application of GA and PSO Tuned Fuzzy Controller for AGC of Three Area Thermal-Thermal-Hydro Power System,**” *Int. J. Comput. Theory Eng.*, vol. 2, Apr. 2010.
- [34] H. Shabani, B. Vahidi, and M. Ebrahimpour, “**A robust PID controller based on imperialist competitive algorithm for load-frequency control of power systems,**” *ISA Trans.*, vol. 52, no. 1, pp. 88–95, 2013, doi: 10.1016/j.isatra.2012.09.008.
- [35] E. S. Ali and S. M. Abd-Elazim, “**BFOA based design of PID controller for two area Load Frequency Control with nonlinearities,**” *Int. J. Electr. Power Energy Syst.*, vol. 51, pp. 224–231, 2013, doi: 10.1016/j.ijepes.2013.02.030.
- [36] Saini Narendra and Ohri Jyoti, “**Load Frequency Control of Multi-area Thermal Power System Using Grey Wolf Optimization,**” in *Control and Measurement Applications for Smart Grid*, 2022, pp. 347–357.
- [37] S. Mirjalili, “**SCA: A Sine Cosine Algorithm for solving optimization problems,**” *Knowledge-Based Syst.*, vol. 96, pp. 120–133, Mar. 2016, doi: 10.1016/j.knsys.2015.12.022.
- [38] M. N. Alam, “**Particle Swarm Optimization: Algorithm and its Codes in MATLAB Networked Microgrids View project Cochlear Implant View project**”, doi: 10.13140/RG.2.1.4985.3206.
- [39] S. Thede, “**An introduction to genetic algorithms,**” 2004. [Online]. Available: <https://www.researchgate.net/publication/228609251>
- [40] S. Mirjalili, S. M. Mirjalili, and A. Lewis, “**Grey Wolf Optimizer,**” *Adv. Eng. Softw.*, vol. 69, pp. 46–61, 2014, doi: 10.1016/j.advengsoft.2013.12.007.